CRYSTAL GROWTH & DESIGN

Article

pubs.acs.org/crystal

First Steps for the Direct Purification of L-Leu-L-Leu Dipeptide through Co-Crystallization

Paolo Lucaioli,[†] Elisa Nauha,[‡] Ishwar Singh,*[,†] and Nicholas Blagden*[,†]

University of Lincoln, [†]School of Pharmacy, [‡]School of Chemistry, Joseph Banks Laboratories, Green Lane, LN6 7DL, Lincoln, United Kingdom

Supporting Information

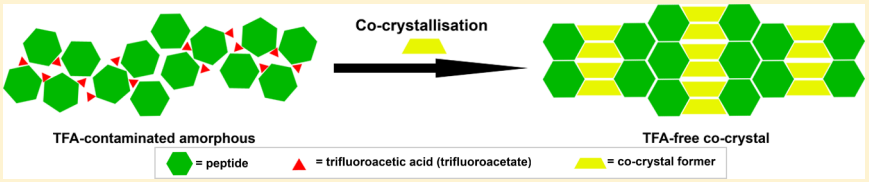

ABSTRACT: Trifluoroacetate salt contamination of peptides represents a challenging issue related to solid phase peptide synthesis and purification because it affects the chemical and biological properties of peptides. Purification of such materials is typically performed through a two-step post-synthetic procedure based on chromatography followed by ion exchange. For the first time, co-crystallization is presented in this study as a possible alternative and advantageous single-step method for the obtaining of TFA-free crystals of a dipeptide. A trifluoroacetate-contaminated L-Leu-L-Leu dipeptide has been used for co-crystallization experiments along with different solid coformers. New multicomponent crystals containing only the title compound and the second co-crystal formers are described in this work. Such results represent a novelty in the field of peptide chemistry and a valid proof for the use of crystal engineering-based method for a combined purification and crystallization strategy.

INTRODUCTION

Biologics might represent the only efficient way to treat some specific diseases but, in many cases, the solid-state form of these entities cannot be easily used in a dosage form due to their questionable physiochemical properties (e.g., stability). Biologics typically exist in the amorphous state with consequent disadvantageous therapeutic and preformulation properties. A possible contemporary solution to this crystallizability issue is the preparation of crystal forms of these molecules using and applying the concepts of crystal engineering and molecular complexes.[1] Hydrophobic peptides can be considered as small prototypes of biologics with a nontoxic, biocompatible, and ecological profile. From a chemical and crystal engineering point of view, their hydrophobic and hydrophilic moieties are very attractive because of the possibility to generate both hydrogen bonded and van der Waals interactions leading to different types of crystal packing landscapes.

An innovative aspect presented in this work is the use of co-crystallization as an alternative method to overcome the problematic removal of unwanted trifluoroacetic acid (TFA) from a synthesized peptide. The presence of such chemical is a common challenge when peptides are synthesized through solid or solution phase peptide synthesis. For example, the final step in the solid phase peptide synthesis (SPPS)[2] is represented by the detachment of the peptide from the resin: this operation is performed using a cleavage cocktail containing a large excess of trifluoroacetic acid, a harmful and polluting strong acid, (pK_a = 0.23), able to cleave the product from the support. TFA binds to the free amino terminal as well as to any positively charged functionality on the side chains of the peptide generating a strong ion pair. Trifluoroacetate salts negatively affect both the physiochemical[3] and the biological[4−6] properties of the product. For this reason, additional purification steps through chromatographic techniques followed by ionic exchange reactions are routinely used to remove this contaminant. A disadvantageous loss in the yield of the peptidic material is unavoidable.

To investigate the possible outcome of purification through co-crystallization, a L-Leu-L-Leu dipeptide was not completely purified after the Fmoc SPPS: the synthesis liquor (containing both the product and the TFA) has been simply evaporated and the recovered material has been lyophilized to obtain a dehydrated peptide. Slow solvent evaporation experiments conducted by using several co-crystal formers along with the dipeptide product show that there is a wide range of possible outcomes (Figure 1): this is due to the establishment of differential crystallization processes involving different chemical species and leading to the formation of adducts with distinct compositions and solubilities. The novel TFA-free multicomponent crystals presented in this paper have been obtained using the nonpurified Leu-Leu dipeptide and 3-aminobenzamide (**LL:3-ABA**), 1H-Pyrazole (**LL:1H-Pyz**), and methanol (**LL:MeOH**) confirming the hypothesis of co-crystallization as an alternative protocol for the removal of

Received: October 31, 2017
Revised: November 27, 2017
Published: December 7, 2017

DOI: 10.1021/acs.cgd.7b01516
Cryst. Growth Des. XXXX, XXX, XXX−XXX

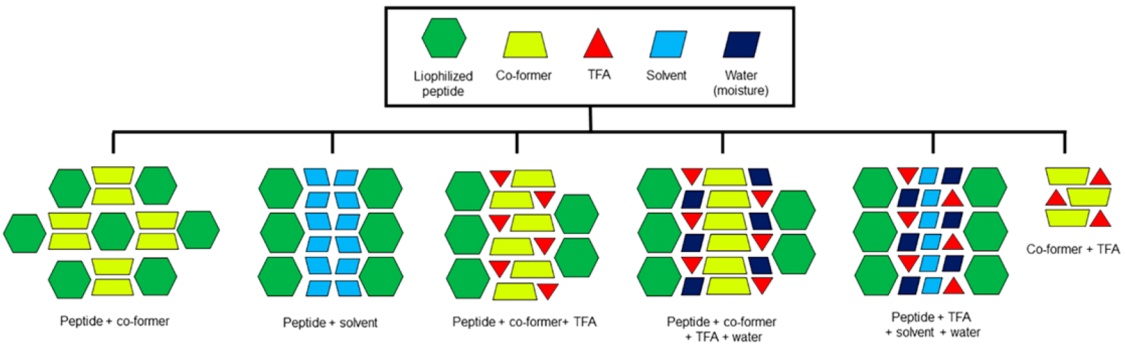

Figure 1. Different multicomponent systems obtained during the co-crystallization screening experiments using the TFA-contaminated L-Leu-L-Leu dipeptide.

trifluoroacetic acid. Crystal products containing TFA will be described in a following paper[7] to highlight the variety of outcomes.

With regard to the crystal science of dipeptides, they typically crystallize in multilayered structures with alternating hydrophobic and hydrophilic layers:[8] the latter are represented by two-dimensional sheets generated through head-to-tail hydrogen bonds involving two of the three amino H atoms and the carboxylate functionality at the other terminal,[9] while the third one is generally involved in an interaction with an acceptor contained in one of the side chains of a peptide of an adjacent layer.[10,11] A crystal packing problem arises when dipeptides are constituted of two hydrophobic residues: from a crystallographic point of view, amino acids are considered hydrophobic when they have no chemical functionalities involved in strong hydrogen bond interactions except for the amino and carboxylate groups in the polar head.[12] In this case, the side-chains do not contain any H-bond acceptor able to accept the third H atom on the amino-terminal of the dipeptide. With the exception of the L-Met-L-Met peptide (in which the third amino H atom is not used for the crystal structure construction),[13] the hydrogen not involved in the creation of the planar sheet is usually accepted by a molecule of crystallization solvent included in the crystal packing.[14]

The crystal structures of L-Leu-L-Val and L-Leu-L-Leu peptides represent significant examples of such arrangements: differently from other hydrophobic dipeptides, these compounds can generate good quality large crystals (instead of thin needles or plates) that can be easily analyzed. Solvates of both L-Leu-L-Val with methanol (CSD refcode:[15] SUWLIF), ethanol (SWLOL), 2-propanol (JUCSEF01)[16] and L-Leu-L-Leu with isopropanol (HIQWAF),[17] ethanol (JUQQUIV), propanol (JUQQUB), 2-propanol (JUQQUM), a 1-propanol:2-propanol mixture (JUQRAO),[18] and DMSO (YORPEA)[19] have already been reported in the literature. The inclusion of such organic solvent molecules in the crystal packing is fundamental for two reasons: first, the hydroxyl groups are involved in the hydrogen bonded networks and represent a valid solution for the problem related with the third amino H atom. On the other hand, these solvents are contained inside channels running in the hydrophobic layers: structures with such empty spaces would not be stable[20] and the presence of a second compound is needed to fill this voids, creating solid architectures. Inclusion compounds of water[21] (RELWIO), pyridine (YIMWOH), and three different methylpyridines[22] (YIMWUN, YIMXAU, YIMXEI) displaying a similar layered structure have been obtained using the L-leucine tripeptide: this results confirm that the presence of solvents is fundamental for the crystal packing.

Despite the importance of their role, the presence of a second component that is liquid at room temperature is usually considered a source of practical problems (e.g., molecular disorder, characterization issues, polymorphism). An additional disadvantage is the questionable stability of solvate forms. This aspect is vital when biological molecules are used for the formulation of pharmaceutical products that must maintain the same properties under different environmental factors such as temperature, pressure, humidity, etc. Co-crystallization experiments using various solid coformers at room temperature have been performed to investigate the possibility to obtain similar stable crystal structures and to analyze the influence of these molecules in the packing architectures.

Interesting cases of hydrophobic dipeptides crystallized without solvent or as hydrates are represented by nanotube formations with different space groups and with hydrophobic[23−25] or hydrophilic[26,27] channels. A novel structure (**LLhex**) belonging to the latter type has been obtained while trying to co-crystallize the title compound with 4-dimethylamino pyridine (DMAP) and will be discussed in this article.

EXPERIMENTAL SECTION

Dipeptide Synthesis. The L-Leu-L-Leu dipeptide (Figure S1) was synthesized through manual Fmoc solid phase peptide synthesis using Fmoc-NH Leu-OH protected amino acid (Merck Millipore) and 2-chlorotrityl chloride resin (Iris Biotech GmBH). The initial manufacturer loading was 1.60 mmol/g. The resin initial loading has been carried out using 4 equiv of protected amino acid and 8 equiv of *N,N*-diisopropylethylamine (DIPEA) in dichloromethane. The Fmoc deprotection steps were performed using a 20% solution of piperidine in dimethylformamide (DMF) while protected amino acid (4 equiv), HATU (4 equiv), and *N,N*-diisopropylethylamine (8 equiv) have been used for the coupling reactions in DMF; a 20:5:75 mixture of trifluoroacetic acid, triisopropylsilane, and DCM was the cleavage cocktail (evaporated with a rotavapor). The final product was lyophilized to eliminate and avoid any possible moisture. These treatments lead to the elimination of most of the excess of TFA (boiling point: 72.4 °C) although it is still present in the final compound.

Co-Crystallization Experiments. 3-Aminobenzamide, 1*H*-Pyrazole, Pyrazine and 4-dimethylamino pyridine were obtained from Alfa Aesar and used to prepare equimolar solution of dipeptide and coformer, using methanol (HPLC purity) as solvent. Thirty different coformers have been used for a complete screening. Such molecules have been chosen among the most common coformers widely encountered, and have a wide variety of structural features (e.g., linear, aromatic, heterocyclic), chemical functionalities (i.e., hydrogen bond donors and acceptor), and chemical properties (i.e., acids and bases). The vials containing the filtered solutions were capped with perforated parafilm to allow slow solvent evaporation at a controlled temperature

DOI: 10.1021/acs.cgd.7b01516
Cryst. Growth Des. XXXX, XXX, XXX−XXX

Table 1. Experimental Details

	(LL:3-ABA)	(LL:1H-Pyz)	(LL:MeOH)	(LLhex)
chemical formula	$C_{12}H_{24}N_2O_3 \cdot C_7H_8N_2O$	$C_{12}H_{24}N_2O_3 \cdot C_3H_4N_2$	$C_{12}H_{24}N_2O_3 \cdot 1.5(CH_4O)$	$C_{12}H_{24}N_2O_3$[+solvent]
M_r	380.48	312.41	292.39	244.33
crystal system, space group	Monoclinic, $P2_1$	Monoclinic, $P2_1$	Monoclinic, $P2_1$	Hexagonal, $P6_1$
a (Å)	5.5139 (3)	5.3441 (2)	10.5689 (5)	23.2661 (13)
b (Å)	22.4965 (13)	13.8666 (6)	13.6495 (6)	23.2661 (13)
c (Å)	16.3133 (9)	12.1977 (5)	12.4721 (5)	5.3295 (3)
α (deg)	90	90	90	90
β (deg)	92.344 (4)	90.514 (2)	107.003 (2)	90
γ (deg)	90	90	90	120
V (Å^3)	2021.9 (2)	903.87 (6)	1720.58 (13)	2498.4 (3)
Z	4	2	4	6
m (mm^{-1})	0.72	0.66	0.69	0.56
Crystal size (mm)	0.14 × 0.04 × 0.04	0.49 × 0.27 × 0.08	0.36 × 0.19 × 0.11	0.61 × 0.10 × 0.06
T_{min}, T_{max}	0.676, 0.753	0.542, 0.754	0.606, 0.753	0.531, 0.753
No. of measured reflections measured	14809	26545	17122	11658
No. of independent reflections	7019	3559	3395	2942
No. with [$I > 2s(I)$]	5347	3395	6054	2109
R_{int}	0.058	0.054	0.039	0.081
(sin $q/l)_{max}$ (Å^{-1})	0.596	0.617	0.603	0.603
$R[F^2 > 2s(F^2)]$	0.050	0.032	0.045	0.071
$wR(F^2)$	0.106	0.079	0.122	0.187
S	1.03	1.05	1.07	1.10
No. of reflections	7019	3559	6185	2942
No. of parameters	559	245	422	170
No. of restraints	17	6	11	5
Dρ_{max}, Dρ_{min} (e Å^{-3})	0.17, −0.19	0.13, −0.16	0.27, −0.21	0.15, −0.19
Absolute structure parameter	−0.06 (19)	−0.07 (8)	0.10 (6)	0.1 (3)

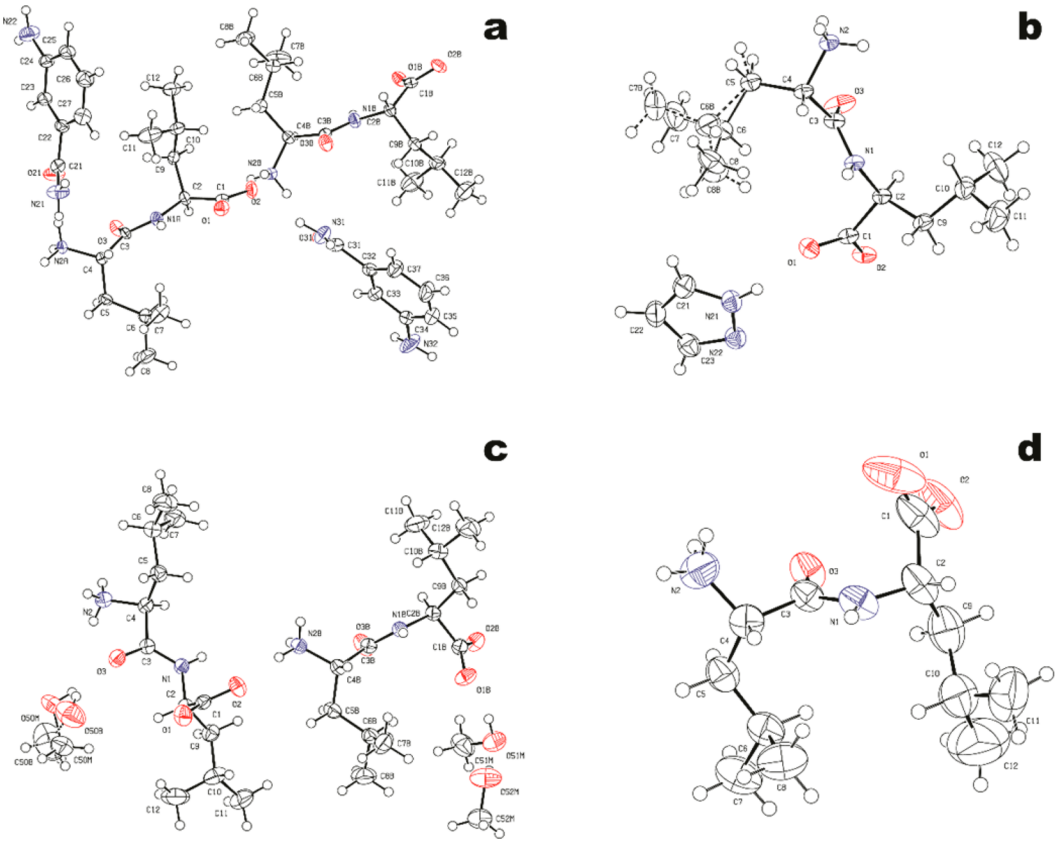

Figure 2. Asymmetric unit of LL:3-ABA (a), LL:1h-Py (b), LL:MeOH (3), and LLhex (d).

DOI: 10.1021/acs.cgd.7b01516
Cryst. Growth Des. XXXX, XXX, XXX−XXX

(20 °C) in an incubator. Crystals with dimensions suitable for single crystal X-ray diffraction were collected from the solution (when possible) or recovered from the dry material. The methanol solvate (**LL:MeOH**) has been obtained when trying to co-crystallize the dipeptide with pyrazine as a coformer while the hexagonal nanotube structure **LLhex** was crystallized using a 1:1 solution with 4-dimethylaminopyridine.

X-ray Diffraction. Single crystals suitable for X-ray diffraction measurements were mounted on MiTeGen Dual-Thickness Micro-Mounts and analyzed using a Bruker D8 Venture diffractometer with a Photon detection system. Unit cell measurements and data collections were performed at 173 K using a Cu Kα radiation (λ = 1.54056 Å). Crystal data and refinement parameters are presented in Table 1. Structure solutions were carried out by direct methods and refinement with SHELXL[28] was finished using the ShelXle[29] software. All non-hydrogen atoms were found from electron density map and refined with fixed bond distances and thermal parameter riding on the parent atom. Highly disordered electron density inside the channel of **LLhex** was processed using Platon Squeeze.[30]

Asymmetric Units. The asymmetric units of the four multi-component systems are shown in Figure 2. **LL:3-ABA**, **LL:1H-Py**, and **LL:MeOH** crystallize in the $P2_1$ space group with a variable number of components. Structures containing 3-aminobenzamide (Figure 2a) and methanol (Figure 2b) are composed of two independent molecules of dipeptide along with two and three molecules of co-crystal former, respectively. The dipeptide molecule in **LL:1H-Py** shows one disordered isobutyl side chain with partial occupancies of 83:17%; disorder has also been found in one of the methanol in **LL:MeOH** (occupancies: 65:35%). **LL:(DMAP)** crystallizes in the hexagonal crystal system with a $P6_1$ space group. The asymmetric unit shown in the present work (Figure 2d) contains just one molecule of dipeptide although additional electron density has been found inside the channel: the structure was squeezed during the refinement process to improve the quality of the final result.

The molecular conformation of the dipeptide molecules in the different structures can be described using the θ = C_1^{β}-C_1^{α}··· C_2^{α}-C_2^{β} torsion angle (Figure 3). This parameter is a useful descriptor of the

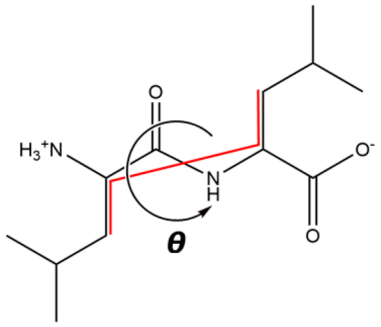

Figure 3. Graphical illustration of θ torsion angle in a dipeptide molecule.

relative position of the side chains with respect to the plane generated by the peptide bond in the molecule backbone. As reported by Görbitz,[27] most of the dipeptides contained in the Cambridge Structural Database are characterized by a $|\theta| > 90°$: this means that the side chains are usually pointing in almost opposite directions. A comparison of $|\theta|$ (Figure 4) of the title compounds reveal a significant difference between the here reported structures: molecules in LL:3-ABA, LL:1H-Py, and LL:MeOH show values that are consistent with the general tendency, while LL:(DMAP) stands out for a remarkably lower angle: this represent a completely different conformation of the dipeptide with the two isobutyl chains positioned on the same side of the peptide bond plane.

RESULTS AND DISCUSSION

Multilayered Structures. The dipeptides molecules in the structures **LL:3-ABA**, **LL:1H-Pyz**, and **LL:MeOH** self-assemble in the *ac*- or *ab*-plane to generate two-dimensional sheets with varying features that are related to the specific hydrogen bonded networks created in each structure. The two isobutyl side chains of each leucine residue extend in opposite directions above and below the plane. Neighboring sheets stack on top of each other creating multilayered architectures in which there is an alternation of hydrophilic layers represented by the dipeptide backbones and hydrophobic regions formed by the side chains of two flanking sheets. The above-described orientation of the nonpolar side chains creates channels of different sizes on both sides of each sheet: these empty spaces host a variable number of coformer (or solvent) molecules (Figure 5).

Two-Dimensional Sheets. The two-dimensional sheet of **LL:3-ABA** in the *ac*-plane is generated exclusively via head-to-tail interactions between the amino and the carboxylate groups of the two independent dipeptide molecules: the internal amidic groups of the peptide bonds are not involved in conventional hydrogen bonds. Only two of the three amino H atoms are involved in the contacts between the neighboring peptide molecules: the first one creates a single H-bond with one of the carboxylic oxygens of a adjacent dipeptide while the second one forms a bifurcated contact with the COO^- group of a third molecule (Figure 6a).

The self-assembly of the dipeptide molecules for the **LL:1H-Pyz** structure is different in that the functionalities of the internal peptide bonds are involved in the formation of the sheet. Two of the three amino H atoms generate strong head-to-tail hydrogen bonds by interacting with the O^- atoms of the C-termini of two neighboring peptides (red in Figure 6b). The internal peptide bond functional groups hydrogen bond with the charged terminals: the N−H group generates a N−H···O^- H-bond with a carboxylate O atom (blue in Figure 6b), while the carbonyl acts as an acceptor for an amino H atom of a adjacent amino-terminal (orange in Figure 6b).

Figure 6c shows the sheet of the **LL:MeOH** structure generated through a hydrogen bonded network that is an intermediate between the previous two. The amino terminals of the two independent dipeptide molecules in the asymmetric unit act as hydrogen bond donors for head-to-tail charge-assisted H-bonds with the carboxylate groups of the neighboring molecules (red contacts in Figure 6c). One of the two dipeptides (yellow in Figure 6c) generates the same interactions described for the **LL:3-ABA**, while the other one (magenta in Figure 3c) uses the N-terminus to create two single N−H···O^- interactions with the C-terminals of two adjacent dipeptides. In this case just the N−H group of the internal peptide bond of each dipeptide participates in a N−H···O^- hydrogen bond (blue in Figure 6c) with one of the carboxylate O atoms of a subsequent molecule.

Three-Dimensional Stacking of Sheets. The channels of **LL:3-ABA** can host 2 parallel chains of coformer molecules (Figure 7c), each one composed of only one type of the two molecules of coformer in the asymmetric unit: these strands are generated through a C═O···H−N interaction between the amide functional groups (magenta in Figure 7c). The two parallel chains are connected through a weak (bond angle = 119.30°) N−H···O hydrogen bond between the amino group of just one type of 3-aminobenzamide molecule and the

DOI: 10.1021/acs.cgd.7b01516
Cryst. Growth Des. XXXX, XXX, XXX−XXX

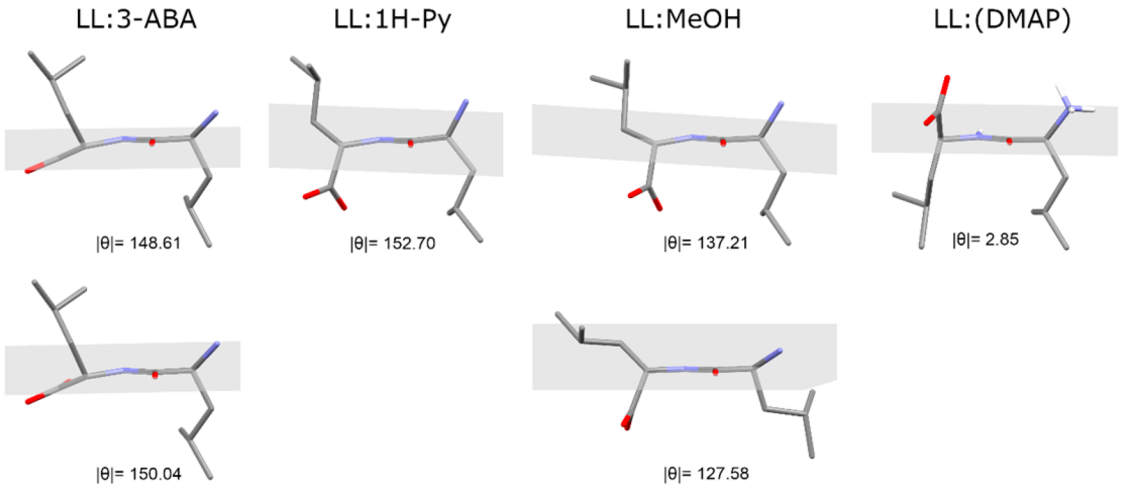

Figure 4. $|\theta|$ torsion angle values [°] of the different dipeptide molecules in the asymmetric units. The gray plane is the one generated by the amidic peptide bond.

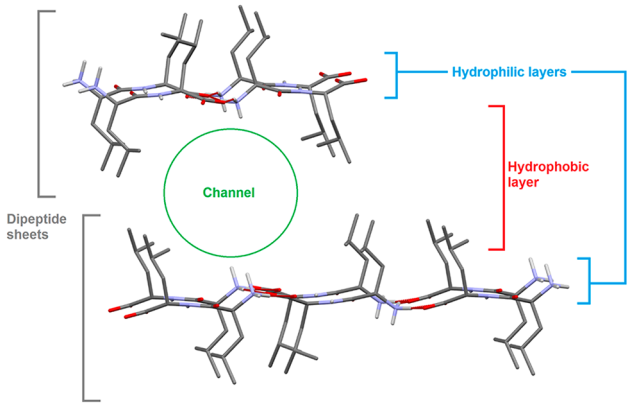

Figure 5. General packing scheme for LL:3-ABA, LL:1H-Pyz, and LL:MeOH.

carbonyl O atom of the amidic groups on the flanking row (orange in Figure 7c). The meta-position of the chemical functionalities allows the coformers to act as cross-linkers between two adjacent sheets (Figure 7b). The amino group generate a $NH\cdots O^-$ with one of the oxygen atoms of the carboxylic terminal of a dipeptide molecule of one sheet, while on the other side, the amidic functionality generates two different hydrogen bonds: the NH_2 is involved in a $NH\cdots O^-$ contact with one of the carboxylic O atoms of a peptide C-terminus and the C═O acts as a hydrogen bond acceptor for the third amino H atom of a peptide N-terminus (the only one not used to generate the sheet).

Because of the different orientation of the dipeptide molecules in the sheet, the hydrophobic isobutyl chains are closer in **LL:1H-Pyz**: this generates channels of smaller size (Figure 8a) that can host just one single row of 1*H*-Pyrazole molecules (not interacting between each other). The coformer contains both an acceptor (N atom) and a donor (N−H group) in its molecule and both are involved in the formation of hydrogen bonds: the acceptor generates a $N\cdots H-N^+$ interaction with the amino H atom not included in the H-bonded network creating the sheet; the N−H functionality interact via single hydrogen bond with one of the O atoms of the C-terminus of a second adjacent dipeptide molecule (Figure 8b).

The particular arrangement of the dipeptide molecules and the complex hydrogen bonded network in **LL:MeOH** implicate a wavy conformation of the two-dimensional sheets (Figure 9a) with a consequent closer approach between the isobutyl side chains. This feature causes a reduction of the channels in the hydrophobic layers that, in this case, only contain few small molecules of crystallization solvent. Three different molecules of methanol interact with the hydrophilic layers, acting as bridges between adjacent molecules: the disordered one (blue in Figure 9b) acts as both an acceptor (for a N^+-H···O H-bond with the amino terminal of a dipeptide) and a donor (for a O−

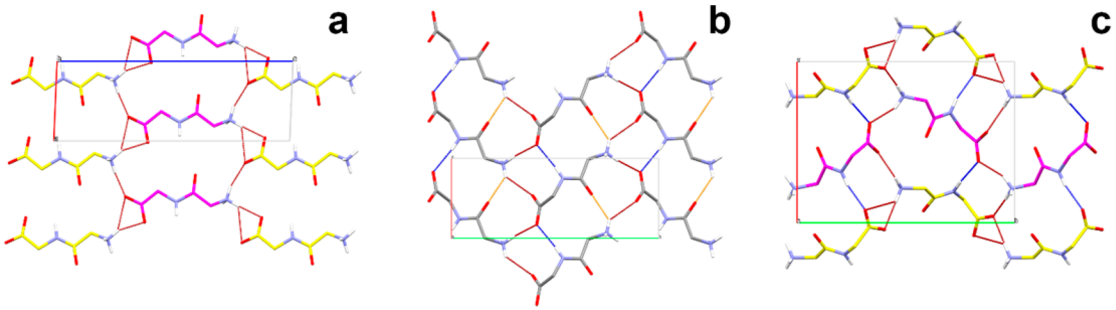

Figure 6. (a) Two-dimensional sheet of LL:3-ABA on the *ac*-plane. (b) Hydrogen bonded network generating the LL:1-Pyz sheet. (c) Hydrogen bonded network generating the sheet of LL:MeOH on the *ab*-plane. The two independent dipeptide molecules of the asymmetric unit are shown in different colors. Isobutyl side chains are not shown for clarity.

DOI: 10.1021/acs.cgd.7b01516
Cryst. Growth Des. XXXX, XXX, XXX−XXX

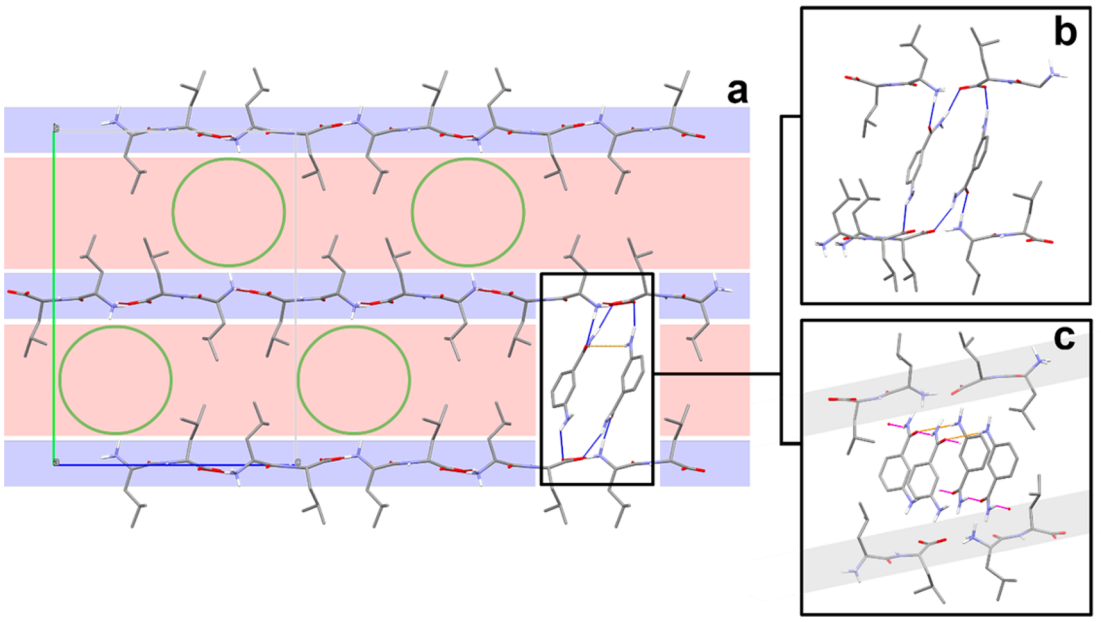

Figure 7. (a) Multilayered structure generated by stacks of dipeptides sheets along the *b*-axis. Each channel (green) can host two coformer molecules that act as cross-linkers between two parallel sheets (b and c).

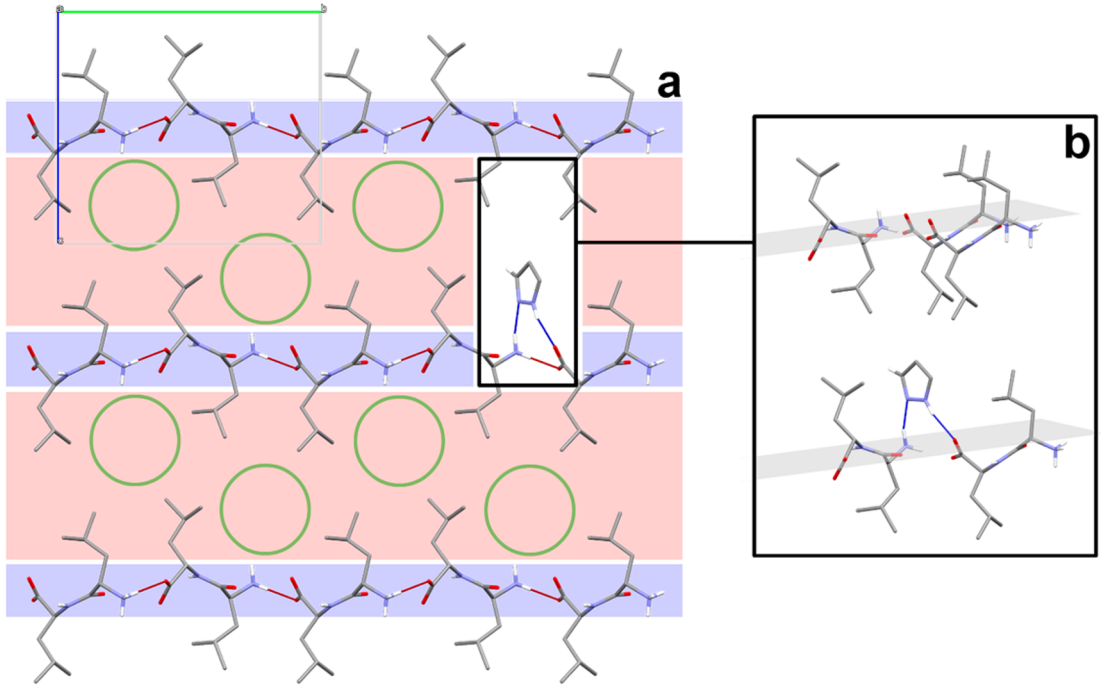

Figure 8. (a) Stacking of sheets for LL:1H-Pyz and (b) interactions involving the coformer.

H···O═C interaction with the carbonyl of the peptide bond of a flanking molecule). The other two molecules of solvent cooperate tighter to create a "bridge effect" between two facing L-leucine-L-leucine: also in this case one of them (magenta in Figure 9b) acts as both an acceptor (giving the same interaction of the disordered one) and a donor (O−H···H hydrogen bond with the third molecule of MeOH, green in Figure 9b), while the other one (green in Figure 9b) is involved in a bifurcated H···O^- contact with the carboxy-terminal of a dipeptide.

Nanotube Structure. The crystal packing of **LL:hex** can be included in the reported cases of nanotubes obtained using hydrophobic dipeptides.[27] This structure crystallizes in $P6_1$. The dipeptides are connected into chains by strong bifurcated head to tail hydrogen bonds (N^+-H···$^-$O−C, red in Figure 10b) resulting in helices contain six molecules per turn (Figure 10a). Each carboxy-terminal act as a bridge connecting flanking parallel spirals generating two interactions: a strong charge-assisted H-bond with the N-terminus (orange in Figure 10b), and another with the N−H group of the internal peptide bond (blue in Figure 10b). The hydrophilic channel runs along the *c* axis surrounded by hydrophobic regions represented by the isobutyl chains.

A L-Leu-L-Leu dipeptide nanotube formation has already been reported (CSD refcode: IDUZOW)[27] but this structure

DOI: 10.1021/acs.cgd.7b01516
Cryst. Growth Des. XXXX, XXX, XXX−XXX

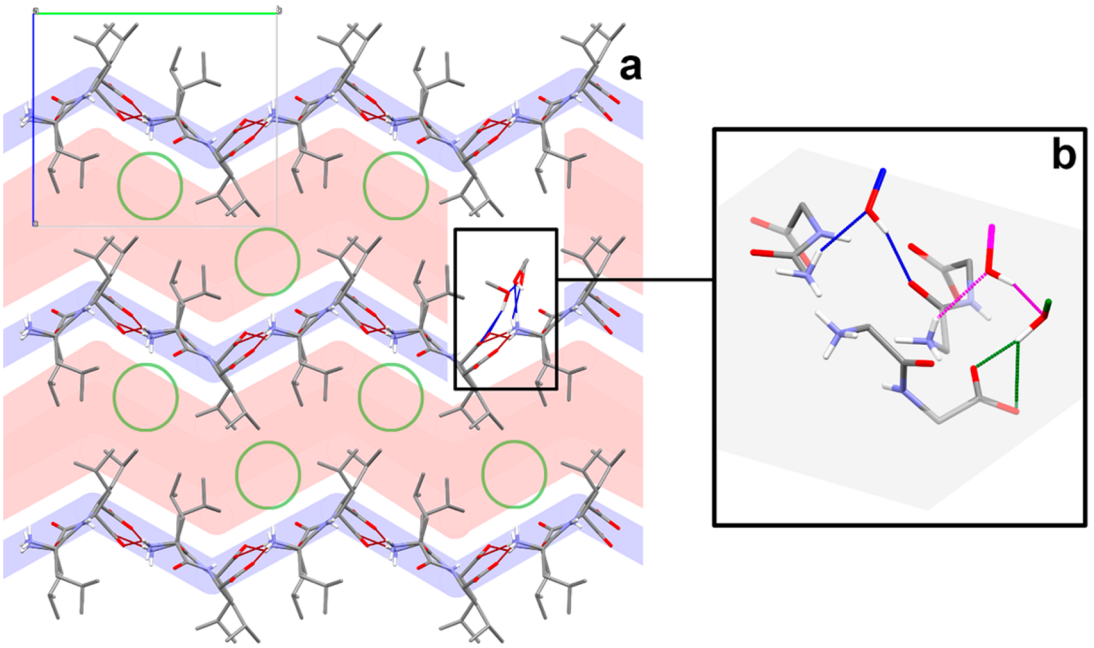

Figure 9. (a) Multilayered stacking of LL:MeOH with molecules of solvents (b).

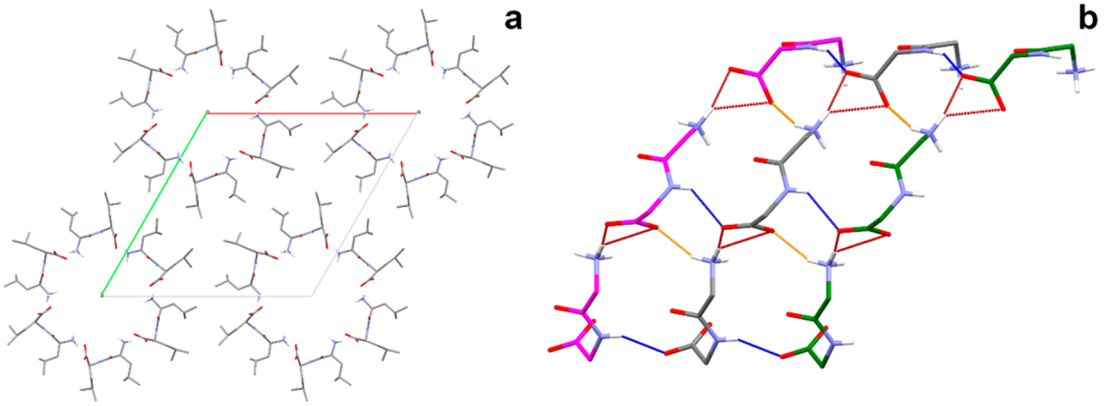

Figure 10. (a) Unit cell and molecular packing of LLhex. (b) Hydrogen bonded network: molecules of dipeptide belonging to the same spiral chain are shown in different colors. Isobutyl side chains are not shown for clarity.

crystallizes in $P2_12_12_1$ with four molecules per turn in the helices. The L-Phe-L-Phe hexagonal structure described by Görbitz in the same paper (IFABEW) is highly similar to **LLhex** (Figure S8). The hydrophilic channel is around 10 Å in diameter comprising 15% of the unit cell volume and it likely contains methanol and water (SI for details).

CONCLUSION

The success in obtaining TFA-free multicomponent crystals represents a proof of concept for the use of crystal engineering as an alternative purification method for freshly synthesized peptides. Further studies aiming to probe the kinetics and thermodynamics behind the differential crystallization mechanisms are the next step. Such investigations will bring about the control of the process and allow a combined purification and crystallization of biologics in a single step, saving time and material.

In the previously reported case of studies on the crystallization of hydrophobic peptides, the impact of TFA was not investigated since the dimers used for the experiments were obtained commercially with a high grade of purity. However, structures reported in the literature show the ability of such compounds to generate well-defined crystal packings in which molecules of different solvents play a fundamental role for the stability of the dipeptide scaffolding, leading to a crystal engineering solution.

The structures of the present study demonstrate that the use of solid (at room temperature) coformers represents a valid alternative for the generation of crystal structures that are consistent with the already reported ones, in which the solvent molecules have been completely replaced. The comparison of the different multilayered packings shows the possibility to have channels of variable size according to the coformers used in the co-crystallization experiments. In **LL:3-ABA** the meta-position of the two chemical functionalities in the 3-aminobenzamide molecule leads the coformer to act as a bridge connecting two parallel sheets, introducing an additional anchoring point in the multilayered stacking. This leads to 3D H-bonded architecture that is more stable than an assembly of 2D-sheets interacting through weaker interactions.

LLhex can be included in the family of hydrophilic nanotube structures of hydrophobic dipeptides (also known as "the Phe-

DOI: 10.1021/acs.cgd.7b01516
Cryst. Growth Des. XXXX, XXX, XXX−XXX

Phe class"[31]). Such self-assembling systems are considered useful models from both a biological and chemical perspective. On one side they can be seen as valid models for ion channels or transmembrane pore assemblies.[32] Also, similar microporous materials attract attention and have been largely used to investigate the relative sorption ability[33−35] for gas storage and other applications.

■ ASSOCIATED CONTENT

Supporting Information

The Supporting Information is available free of charge on the ACS Publications website at DOI: 10.1021/acs.cgd.7b01516.

Pictures showing the different possible outcomes of the co-crystallization screening, hydrogen bonded networks comparison between two-dimensional sheet of L-Leu-L-Leu dipeptide and L-Leucine, crystal packing analysis of LLhex, IFABEW, and IDUZOW nanotubes (PDF)

Accession Codes

CCDC 1579695−1579698 contain the supplementary crystallographic data for this paper. These data can be obtained free of charge via www.ccdc.cam.ac.uk/data_request/cif, or by emailing data_request@ccdc.cam.ac.uk, or by contacting The Cambridge Crystallographic Data Centre, 12 Union Road, Cambridge CB2 1EZ, UK; fax: +44 1223 336033.

■ AUTHOR INFORMATION

Corresponding Authors

*E-mail: isingh@lincoln.ac.uk.

*E-mail: nblagden@lincoln.ac.uk.

ORCID

Elisa Nauha: 0000-0001-9784-8988

Nicholas Blagden: 0000-0001-5363-6748

Notes

The authors declare no competing financial interest.

■ ACKNOWLEDGMENTS

Funding for PL provided by the University of Lincoln, School of Pharmacy.

■ REFERENCES

(1) Duggirala, N. K.; Perry, M. L.; Almarsson, Ö.; Zaworotko, M. J. *Chem. Commun.* **2016**, *52*, 640−655.

(2) Chan, W. C.; White, P. D. *Fmoc solid phase peptide synthesis: a practical approach*; Oxford University Press, 2000.

(3) Shen, C. L.; Fitzgerald, M. C.; Murphy, R. M. *Biophys. J.* **1994**, *67*, 1238−1246.

(4) Cornish, J.; Callon, K. E.; Lin, C. Q.-X.; Xiao, C. L.; Mulvey, T. B.; Cooper, G. J. S.; Reid, I. R. *Am. J. Physiol. - Endocrinol. Metab.* **1999**, *277*.

(5) Tipps, M. E.; Iyer, S. V.; John Mihic, S. *Neuropharmacology* **2012**, *63*, 368−373.

(6) Ma, T. G.; Ling, Y. H.; McClure, G. D.; Tseng, M. T. *J. Toxicol. Environ. Health* **1990**, *31*, 147−158.

(7) Lucaioli, P.; Nauha, E.; Singh, I.; Blagden, N. *in preparation*.

(8) Görbitz, C. H.; Etter, M. C. *Int. J. Pept. Protein Res.* **1992**, *39*, 93−110.

(9) Prasad, G. S.; Vijayan, M. *Int. J. Pept. Protein Res.* **1990**, *35*, 357−364.

(10) Eggleston, D. S. *Acta Crystallogr., Sect. C: Cryst. Struct. Commun.* **1984**, *40*, 1250−1252.

(11) Görbitz, C. H.; Backe, P. H. *Acta Crystallogr., Sect. B: Struct. Sci.* **1996**, *52*, 999−1006.

(12) Görbitz, C. H. *Crystallogr. Rev.* **2015**, *21*, 160−212.

(13) Stenkamp, R. E.; Jensen, L. H. *Acta Crystallogr., Sect. B: Struct. Crystallogr. Cryst. Chem.* **1975**, *31*, 857−861.

(14) Görbitz, C. H. *Acta Crystallogr., Sect. C: Cryst. Struct. Commun.* **1999**, *55*, 2171−2177.

(15) Groom, C. R.; Bruno, I. J.; Lightfoot, M. P.; Ward, S. C. *Acta Crystallogr., Sect. B: Struct. Sci., Cryst. Eng. Mater.* **2016**, *72*, 171−179.

(16) Görbitz, C. H.; Torgersen, E. *Acta Crystallogr., Sect. B: Struct. Sci.* **1999**, *55*, 104−113.

(17) Görbitz, C. H. *Acta Crystallogr., Sect. C: Cryst. Struct. Commun.* **1999**, *55*, 670−672.

(18) Görbitz, C. H. *Acta Chem. Scand.* **1998**, *52*, 1343−1349.

(19) Mitra, S. N.; Subramanian, E. *Biopolymers* **1994**, *34*, 1139−1143.

(20) Kitaigorodskii, A. I. *Organic Chemical Crystallography*; Consultants Bureau: New York, 1961.

(21) Go, K.; Parthasarathy, R. *Biopolymers* **1995**, *36*, 607−614.

(22) Burchell, T. J.; Soldatov, D. V.; Enright, G. D.; Ripmeester, J. A. *CrystEngComm* **2007**, *9*, 922.

(23) Görbitz, C. H.; Gundersen, E. *Acta Crystallogr., Sect. C: Cryst. Struct. Commun.* **1996**, *52*, 1764−1767.

(24) Görbitz, C. H. *Acta Crystallogr., Sect. B: Struct. Sci.* **2002**, *58*, 849−854.

(25) Henrik Görbitz, C. *New J. Chem.* **2003**, *27*, 1789−1793.

(26) Görbitz, C. H. *Acta Crystallogr., Sect. E: Struct. Rep. Online* **2004**, *60*, o626−o628.

(27) Görbitz, C. H. *Chem. - Eur. J.* **2001**, *7*, 5153−5159.

(28) Sheldrick, G. M. *Acta Crystallogr., Sect. C: Struct. Chem.* **2015**, *71*, 3−8.

(29) Hübschle, C. B.; Sheldrick, G. M.; Dittrich, B. *J. Appl. Crystallogr.* **2011**, *44*, 1281−1284.

(30) Spek, A. L. *Acta Crystallogr., Sect. C: Struct. Chem.* **2015**, *71*, 9−18.

(31) Görbitz, C. H. *Chem. - Eur. J.* **2007**, *13*, 1022−1031.

(32) Hartgerink, J. D.; Clark, T. D.; Ghadiri, M. R. *Chem. - Eur. J.* **1998**, *4*, 1367−1372.

(33) Soldatov, D. V.; Moudrakovski, I. L.; Ripmeester, J. A. *Angew. Chem., Int. Ed.* **2004**, *43*, 6308−6311.

(34) Soldatov, D. V.; Moudrakovski, I. L.; Grachev, E. V.; Ripmeester, J. A. *J. Am. Chem. Soc.* **2006**, *128*, 6737−6744.

(35) Moggach, S. A.; Görbitz, C. H.; Warren, J. E.; Ruf, M.; Jameson, C. J.; Pulham, C. R.; Sawyer, L.; Taylor, R.; Streek, J.; van de Wood, P. A. *CrystEngComm* **2010**, *12*, 2322.

DOI: 10.1021/acs.cgd.7b01516
Cryst. Growth Des. XXXX, XXX, XXX−XXX